Pergamon

Geochimica et Cosmochimica Acta, Vol. 66, No. 22, pp. 3873–3885, 2002

0016-7037/02 $22.00 + .00

PII S0016-7037(02)00974-2

Bonding of methyl mercury to reduced sulfur groups in soil and stream organic matter as determined by X-ray absorption spectroscopy and binding affinity studies

JIN QIAN,[1,2] ULF SKYLLBERG,[1,*] WOLFGANG FRECH,[2] WILLIAM F. BLEAM,[3] PAUL R. BLOOM,[4,5] and PIERRE EMMANUEL PETIT[5]

[1]Department of Forest Ecology, Swedish University of Agricultural Science, S-901 83 Umed, Sweden
[2]Department of Chemistry, Umeå University, S-901 83 Umeå, Sweden
[3]Department of Soil Science, University of Wisconsin, Madison, Wisconsin 53706, USA
[4]Department of Soil, Water and Climate, University of Minnesota, St. Paul, Minnesota 55108, USA
[5]European Synchrotron Radiation Facility, BP 220, F-38043 Grenoble Cedex, Grenoble, France

(*Received December* 13, 2001; *accepted in revised form May* 17, 2002)

Abstract—We combined synchrotron-based X-ray absorption near edge structure (XANES) spectroscopy, extended X-ray absorption fine structure (EXAFS) spectroscopy and binding affinity studies to determine the coordination, geometry, and strength of methyl mercury, CH_3Hg (II), bonding in soil and stream organic matter. Samples of organic soil (OS), potentially soluble organic substances (PSOS) from the soil, and organic substances from a stream (SOS) draining the soil were taken along a short "hydrological transect." We determined the sum of concentrations of highly reduced organic S groups (designated Org-S_{RED}), such as thiol (RSH), disulfane (RSSH), sulfide (RSR), and disulfide (RSSR), using sulfur *K*-edge XANES. Org-S_{RED} varied between 27% and 64% of total S in our samples. Hg L_{III}-edge EXAFS analysis were determined on samples added CH_3Hg (II) to yield CH_3Hg (II)/Org-S_{RED} ratios in the range 0.01–1.62. At low ratios, Hg was associated to one C atom (the methyl group) at an average distance of 2.03 ± 0.02 Å and to one S atom at an average distance of 2.34 ± 0.03 Å, in the first coordination shell. At calculated CH_3Hg(II)/Org-S_{RED} ratios above 0.37 in OS, 0.32 in PSOS, and 0.24 in SOS, the organic S sites were saturated by CH_3Hg^+, and O (and/or N) atoms were found in the first coordination shell of Hg at an average distance of 2.09 ± 0.01 Å. Based on the assumption that RSH (and possibly RSSH) groups take part in the complexation of CH_3Hg^+, whereas RSSR and RSR groups do not, approximately 17% of total organic S consisted of RSH (+ RSSH) functionalities in the organic soil. Corresponding figures for samples PSOS and SOS were 14% and 9%, respectively. Competitive complexation of CH_3Hg^+ by halide ions was used to determine the average binding strength of native concentrations of CH_3Hg (II) in the OS sample. Using data for Org-S_{RED}, calculated surface complexation constants were in the range from $10^{16.3}$ to $10^{16.7}$ for a model RSH site having an acidity constant of mercaptoacetic acid. These values compare favorably with identically defined stability constants (log K_1) for the binding of methyl mercury to thiol groups in well-defined organic compounds. *Copyright © 2002 Elsevier Science Ltd*

1. INTRODUCTION

Atmospheric deposition of anthropogenic mercury is a large-scale environmental problem at northern latitudes. In areas dominated by wetlands, organic soils, and humic surface waters, high concentrations of the very toxic form of Hg, methyl mercury, are formed (Hurley et al., 1995; St. Louis et al., 1996) and subsequently accumulated in higher biota. This has led authorities to discourage people to regularly eat fish from 40,000 lakes in Sweden alone (Håkansson, 1996). Despite extensive research (Watras and Huckabee, 1994; Porcella et al., 1995), there is still very limited knowledge about factors controlling biological and chemical transformations of various Hg forms and mechanisms behind accumulation in organisms (Zillioux et al., 1993; Vaithiyanathan et al., 1996).

Limited knowledge about the chemical bonding of Hg^{2+} and CH_3Hg^+ in soil organic matter (SOM) has hampered mechanistic research about central processes such as methylation of Hg^{2+} to CH_3Hg^+, demethylation of CH_3Hg^+ and reduction of Hg^{2+} to Hg^0 (Hudson et al., 1994; Vaithiyanathan et al., 1996). Methylation is enhanced in environments with periodic variations of reduced and oxidized conditions, such as newly established water reservoirs (Morrison and Therien, 1994) and wetlands (St. Louis et al., 1996). Less is known about factors affecting demethylation rates in soils and waters (Zillioux et al., 1993; Hudson et al., 1994). The identity, coordination and geometry of CH_3Hg (II) and Hg (II) bound in SOM is likely of central importance for both methylation, demethylation and reduction processes. We know from studies of well-defined organic compounds that the Hg–C bond is easier to break in a pseudotetrahedral four-coordination (in triphosphine) than in a linear two-coordination (monophosphine) and that the stability of the Hg–C bond decreases in the order of CH_3HgCl, CH_3HgBr, and CH_3HgI (Barone et al., 1995). Also the bioavailability and detoxification of CH_3Hg are affected by the identity of binding ligands and the coordination number in organic substances (Miller et al., 1989; Moore et al., 1990).

Synchrotron-based EXAFS has been used to obtain structural information on the binding of Hg^{2+} (Xia et al., 1999; Hesterberg et al., 2001) and other divalent trace metals (Xia et al., 1997) in soil humic acids and soil organic matter. There is, to our knowledge, no EXAFS study on the binding of CH_3Hg (II) in soil organic matter. Xia et al. (1999), and Hesterberg et al. (2001) have shown that Hg^{2+} prefers reduced S to oxygen and nitrogen functional groups in extracted organic substances

* Author to whom correspondence should be addressed (ulf.skylberg@sek.slu.se).

from soil. This finding was further supported by a combined sulfur *K*-edge XANES and adsorption study (Skyllberg et al., 2000), showing that the strength of Hg^{2+} binding in soil organic matter was similar to associations between Hg^{2+} and thiol groups in well-defined organic compounds. Hintelmann et al. (1997) have provided the only estimate on the binding strength of methyl mercury to a soil humic acid. Using a dialysis membrane with a molecular weight cutoff of 500 to separate inorganic CH_3Hg (II) complexes from organic complexes they obtained conditional constants, which only could be explained by a complexation involving reduced organic S groups.

In this paper we present results of the first EXAFS study on methyl mercury in soil and stream organic matter. Results were generated for concentrations of CH_3Hg(II) higher, as well as much lower, than the concentration of highly reduced organic S groups (here designated Org-S_{RED}), the presumptive strongest binding sites. By use of sulfur *K*-edge XANES, we determined the concentration of Org-S_{RED}, presumably representing the sum of thiol (RSH), disulfane (RSSH), organic sulfide (RSR), and organic disulphide (RSSR) functionalities. In our EXAFS experiments, the CH_3Hg (II)/Org-S_{RED} ratio was varied between 0.01 and 1.62 in organic substances from soil and stream. The EXAFS experiments were complemented by a binding affinity study performed at native concentrations of methyl mercury in soil, following the procedure of Skyllberg et al. (2000). Combined with S XANES data, binding affinity data were determined and modeled at a CH_3Hg (II)/Org-S_{RED} ratio as low as 10^{-7}.

2. MATERIALS AND METHODS

2.1. Sampling, Sample Preparation and General Chemical Analyses

Organic samples were collected along a 2 m long "hydrological transect" consisting of an organic peat soil (OS), potentially soluble organic substances from the organic soil (PSOS) and organic substances collected in a stream (SOS, stream organic substances) located 2 m away from the sampling point of the organic soil. The organic soil was sampled at 10–20 cm depth, 10 cm above the ground-water table. The hydrosequence is situated within a 50 ha forested catchment in northern Sweden (Nyänget catchment, Svartberget Research Station, 64° 14' N, 19° 46' E), drained by the stream Kallkällebäcken. Hydrograph separation studies with stabile isotopes, as well as chemical "fingerprints," have shown that laterally moving soil water passing through surface layers of the organic soil contributes significantly to runoff in the stream during spring and autumn high-flow events (Bishop, 1991). This means that dissolved organic substances in the stream to a great extent originates from the organic soil. At the sampling occasion, in the end of spring flood in June, the organic soil solution (collected by high-speed centrifugation) had a pH of 3.7 and the stream pH was 4.5. A soil sample was also collected from a fen peat (FP) of a subalpine environment, but within 5 km from the Atlantic Ocean, at Ifjord in northern Norway. This soil had a pH of 5.7 and a relatively high concentration of total sulfur (2.0%), as compared to samples from the hydrological transect. Soil samples were collected and sealed in double plastic bags following protocols for clean sampling procedure. Soil samples were stored in darkness at 4 °C until freeze-dried (Edwards Modulyo 4k Freeze Dryer) and homogenized by a tungsten carbide ball mill (Retsch, S2, Germany).

Potentially soluble organic substances were gently extracted from fresh organic soil at Svartberget and from the Norwegian fen peat, following a modified version of the method used by Adams and Byrne (1989). A metal-chelating resin was used to release organic substances, which are kept flocculated by Ca^{2+} and Al^{3+} in the soil, at a pH around 6. To each of 10 aliquots of 30 g moist soil, 5.0 g of Chelex 20 (Biorad) and 250 ml Millipore water was added in 500 ml polycarbonate centrifuge bottles. After 12 h of gentle shaking in darkness, the brown-colored supernatant was separated from soil and resin by centrifugation at 22,100 g. The supernatant of the Norwegian fen peat sample was collected, freeze-dried and homogenized by a tungsten carbide ball mill. This sample is henceforth referred to as FPOS. The supernatant of the organic soil was collected in a 500 ml centrifuge bottle and added Al $(NO_3)_3$ (under 5 min of stirring) to yield a total Al concentration of 2 mM. After 1 hour of sedimentation in darkness, the formed Al-organic matter flocculate was separated from the clear solution by centrifugation at 22,100 g. Excess Al $(NO_3)_3$ was removed by equilibrating the flocculate for 30 min with three portions of 100 ml distilled water. The addition of Al^{3+} to the organic extract restored adsorbed Al that was originally keeping the organics flocculated in the organic soil. After each equlibration the suspension was centrifuged and the supernatant discarded. pH in the last centrifugate was 4.0. On average 98% of the soil organic carbon mobilized by the resin was reflocculated by $Al(NO_3)_3$, as determined by absorption at 254 nm. The flocculate was freeze dried and homogenized. This sample is henceforth referred to as PSOS.

Stream water with a concentration of 19 mg total organic C per liter was collected from the Kallkällebäcken stream at Svartberget during spring flood (mid-May) when water moved through the organic soil close to the stream. A container with 25 liter of stream water was added $Al(NO_3)_3$ to yield a total Al concentration of 2 mM, immediately after sampling. During 1 hour of transportation to Umeå the stream water + added Al was mixed and 48% of the organic carbon in the stream water was flocculated. After 12 hours of settling in darkness at 6 °C, the supernatant was decanted from the sediment of flocculate. When 1 liter of solution remained in the containers, the organic flocculate was separated from solution by high-speed centrifugation at 22,100 g for 15 min. Excess $Al(NO_3)_3$, and other salts, were removed by equilibrating the flocculate for 30 min in three portions of 100 ml distilled water. After each equlibration the suspension was centrifuged and the supernatant discarded. pH in the last supernatant was 3.9. The organic flocculate of the stream (SOS) was freeze dried and homogenized.

For all samples total organic carbon and total nitrogen were determined by combustion on an elemental analyzer (Perkin–Elmer, 2400 CHN) and total sulfur was determined on a LECO sulfur analyzer (LECO Corp. MI, USA). Total mercury was determined by cold vapor atomic absorption spectroscopy (CVAAS) after acid digestion, and methyl mercury was extracted and determined by gas chromatography, microwave induced plasma atomic emission spectrometry (GC–MIP–AES) following the procedure described by Qian et al. (2000).

Subsamples from the same freeze-dried samples were used in both XANES and EXAFS experiments. Prior to the EXAFS study methyl mercury hydroxide, dissolved in a minimum of double-distilled water, was added to yield molar CH_3Hg(II)/Org-S_{RED} ratios of 0.01, 0.13, 0.53, 1.08, and 1.62 in the OS sample, 0.01, 0.09, 0.47, 0.95, and 1.41 in PSOS, 0.01, 0.12, 0.47, and 1.19 in SOS and 0.30 in the FPOS sample. High-viscosity suspensions of OS, PSOS, and SOS samples were mixed continuously for 7 days to reach equilibrium. These samples were then freeze dried and pellets were prepared 1–2 hours before each EXAFS experiment. As opposed to drying at 60 °C, neither methyl mercury nor mercury have been shown to be lost from organic samples as an effect of freeze drying (Qian et al., 2000). The FPOS sample was prepared in a similar way 7 days before EXAFS analysis, but was kept moist for the EXAFS analysis. pH in all samples fell in the range from 3.8 to 4.0. A thiol resin was used to prepare a CH_3Hg–SR standard. The resin (Duolite GT73, Rohm and Hass) was equilibrated with a CH_3HgOH solution yielding a CH_3Hg (II) concentration of 2500 mg kg^{-1} on a dry mass basis of the resin. This corresponds to 0.3% saturation of thiol groups by CH_3Hg^+. After 24-hour equilibration, the resin was washed with distilled water three times. A carboxylic resin (200–400 mesh Bio-Rex 70) was used to prepare a CH_3Hg–OOCR standard in the same way, yielding 2500 mg kg^{-1} on a dry mass basis. This corresponds to 0.1% saturation of carboxyl groups by CH_3Hg^+. Both resins were freeze dried and mixed with boron nitride prior to pellets preparation. Besides, red HgS (Merck) was also chosen as a standard without any further preparation than grinding and dilution with boron nitride.

2.2. Hg L_{III} Edge EXAFS Data Collection and Analyses

The FPOS sample containing 15,000 mg methyl mercury kg^{-1} (dry mass of soil) was analyzed at a bending-magnet beam line (X11A) at the National Synchrotron Light Source, Brookhaven National Laboratory (NSLS, Upton, NY, USA). We mounted a moist FPOS sample in 1.5 mm-thick polycarbonate holders with Kapton-tape (CHR-Furon) windows. The Si(111) double-crystal monochromator was detuned by 10%. The detector was a Stern–Heald fluorescence ion chamber filled with Kr gas positioned 90 degrees to the incident beam (Lytle et al., 1984). The sample was placed at a 45-degree angle to the incident beam. The monochromator energy was calibrated with the selenium *K* edge (12,658 eV), which is close to the Hg L_{III} edge (12,284 eV). Typical scans ranged from 200 eV below to 800 eV above the absorption edge. Each EXAFS spectrum represents the merged results from 4 to 10 scans depending on their spectral quality. A high noise level was observed for whole soil samples, which made the extraction of EXAFS spectra impossible.

All soil and stream samples (except the FPOS) and model compounds were analyzed on the undulator beam line ID26 (Gauthier et al., 1999) at the European Synchrotron Radiation Facility (ESRF, Grenoble, France). The machine conditions were 6 GeV electron energy and around 200 mA electron current. A Cr-coated Si mirror allowed removing the high-energy harmonics from the incident x-ray beam. A cryogenically cooled fixed-exit double-crystal monochromator with Si(111) was used, giving an energy resolution less than 1 eV at 12,284 eV. The fluorescence signal was detected with a silicon photodiode and a Ga filter was installed between the sample and the detector to reduce the scattering radiation. Hg L_{III} edge in HgO (12,284 eV) was used to calibrate the monochromator energy. A EXAFS spectrum represents the merged results from 4 to 10 scans (each scan taking approximately 20 min to collect), except for the carboxylic resin sample, for which radiation damage was detected after 2 to 3 scans. This was assessed by a successive change in the features of consecutive spectra, and their first derivatives, for this sample. For other samples no radiation damage was indicated. For one sample [PSOS, CH_3Hg (II)/Org-S_{RED} = 0.47] EXAFS data were collected using a quick-scan procedure. The spectrum for this sample represents a merge from 120 scans, each collected during 40 seconds (from 200 eV below to 800 eV above the Hg L_{III} edge).

The EXAFS spectra were analyzed using the program WinXAS97 (Ressler, 1997). The background was removed by fitting a first order polynomial to the pre-edge region and subtracting the extrapolated polynomial from the entire data set. The edge jump was normalized fitting a zero order polynomial to a chosen post-edge section. E_0 was determined as the maximum of the first derivative. A cubic spline fitting procedure (knots = 6 to 9, k = 3) was applied in order to isolate the fine-structure scattering curve from low frequency background. The extracted EXAFS was then weighted by k^3 in order to enhance the high k region. The EXAFS spectra were Fourier transformed using an unsmoothed window over the k range from 2.5 up to 13.0 $Å^{-1}$ to yield a radial structure function (RSF). A narrower k range (2.5–9.3 $Å^{-1}$) was chosen for the samples with the lowest methyl mercury concentration [CH_3Hg (II)/Org-S_{RED} = 0.01] to eliminate excessively noisy data at the high end of the EXAFS spectra. The range of radial distances chosen in the RSF for fitting analysis isolated the highest amplitude, first-shell peak, normally 1.0 to 2.4 Å. Least-squares fitting was first carried out in R space (fit not shown) followed by a final refinement in k space (unfiltered data) by the fit module in the WinXAS97 program. For cinnabar the coordination number was constrained to 2.00 ± 0.05 (theoretical value = 2.00). For other samples, all parameters except the amplitude reduction factor (S_0^2) were allowed to independently vary (float). In all cases, the maximum number of floating parameters was less than the degrees of freedom. The shift of the edge energy, E_0, was constrained to be equal for atomic shells.

Theoretical EXAFS scattering curves and parameters for first shell Hg–S, Hg–O, and Hg–C bonding were generated by the FEFF-7 computer program (Rehr et al., 1994, Zabinsky et al., 1995). Theoretical structural parameters for Hg–S, Hg–O, and Hg–C bonds in organomercury compounds (Holloway and Melnik, 1995) were used as input for FEFF calculations. The accuracy of these were confirmed by fits of cinnabar (red HgS) compared with its theoretical structure and by model compounds with C–Hg–S coordination in thiol resin and with C–Hg–O coordination in carboxyl resin. The latter two model compounds were used to determine relevant amplitude reduction factors. The S_0^2 determined in thiol resin (0.93) was similar to S_0^2 for Hg–S bonding in cinnabar (0.90). The S_0^2 determined in carboxyl resin was 0.90. For the organic samples (OS, PSOS, SOS, and FPOS), a mixed model of C–Hg–S and C–Hg–O associations was used to fit EXAFS data.

2.3. Sulfur Speciation Analysis Using S *K*-Edge XANES

2.3.1. S K-edge XANES data collection

Freeze-dried samples were pressed into thin films by using a 0.5 mm thick acrylic holder with Mylar film (2.5 μm thick, Chemplex Industries, New York) to reduce the self-absorption effect that commonly occurs for a thick sample with S content higher than 0.3 wt. % (Waldo et al., 1991). Then the sample holder was loaded using a shuttle designed by Weesner et al. (1997). The experiment was carried out on beamline X19A at the National Synchrotron Light Source (NSLS) at Brookhaven National Laboratory (Upton, NY). The incident x-ray energy was typically scanned over the range from 2,462 to 2,500 eV with step size of 0.2 eV. Sodium sulfate was used as reference and the energy was calibrated at 2,482 eV with this compound. The energy drift between samples was corrected for by setting the energy of the sulfate peak to 10.0 eV above that of elemental S (2,472 eV), Waldo et al. (1991). A monochromator consisting of two parallel Si {111} crystals with an entrance slit of 0.5 mm and minimum energy resolution of 2×10^{-4} (~0.5 eV at the sulfur K edge) was used. All spectra were recorded in fluorescence mode using a Stern–Heald ionization detector filled with He gas and positioned 90° to the incident beam (Lytle et al., 1984). The monochromator was detuned 70% at the S K edge in order to reduce fluorescence induced by high-order harmonics (Xia et al., 1998).

2.3.2. XANES data analysis

Each XANES spectrum represents the average of 3 to 12 scans depending on the quality of spectra. SOLVER (Microsoft Excel) was used to deconvolute the XANES spectrum for each sample into pseudo-components by using its least-squares- fitting function. The linear part of the spectral baseline was removed, and the spectrum was normalized prior to fitting. A series of Gaussian peaks was used to represent the $s \rightarrow p$ transitions and two arctangent step functions were used to represent the transition of ejected photoelectrons to the continuum. The energy position of the $s \rightarrow p$ peaks can be used to identify the oxidation states of S, while the peak areas can be transformed into the percentage of total S at different oxidation states in a sample after correcting for the change in absorption cross section with increasing oxidation state (Waldo et al., 1991; Xia et al., 1998).

While such least-squares fits are straightforward, it is necessary to introduce a number of conditions and constraints in order to obtain meaningful fits. Assumptions used in the fitting process are (a) all $s \rightarrow p$ transition peaks are Gaussian and all arctangent function parameters were held constant during fitting of the Gaussian components; (b) at least four major components are present in each spectrum, with additional components added in the fitting process until a satisfactory fitting was obtained; (c) the full width at half-maximum (FWHM) of each Gaussian components for S in low and intermediate oxidation states ($\leq$ 4) was loosely constrained between 0.2 and 1.0 eV, whereas the FWHM of Gaussian components for high-valent S (+5 and +6) was tightly constrained at 1.4 ± 0.2 and 2.2 ± 0.2 eV, respectively (0.2 and 1.0 eV are the uncertainty of the energy calibration; 1.4 and 2.2 eV are the FWHM for sulfonate and sulfate model compounds, respectively). Additional justification and assumptions made for the fitting procedure are given elsewhere (Xia et al., 1998).

In order to convert peak area to atomic percentages, the relative transition probabilities of different sulfur forms must be considered. The $s \rightarrow p$ transition probability should be roughly proportional to the number of 3p vacancies in a simple one-electron model and should increase with increasing valence. Models and unknowns with similar peak energies, and therefore similar oxidation states, are expected to have similar peak areas (Waldo et al., 1991). The plot of peak area vs. peak position shows an approximately linear increase (Xia et al., 1998).

Table 1. Total concentrations of organic C, N, S and reduced organic S (Org-S_{RED}), as determined by XANES

Sample	Org-C g kg^{-1}	N_{TOT} g kg^{-1}	S_{TOT} g kg^{-1}	Org-S_{RED} g kg^{-1}	Org-S_{RED}/Org-C
Organic soil (OS)	493	18.3	4.1	1.9	0.0039
Potentially soluble organic substances (PSOS)	480	22.2	5.2	2.2	0.0046
Stream organic substances (SOS)	427	10.7	4.2	1.6	0.0038
Fen peat (FP)	410	23.3	20	13	0.032
Fen peat organic substances (FPOS)	347	12.3	26	7.1	0.020

We located and weighted the areas of each Gaussian peak obtained from the fitting procedures. The weighted peak areas were then used as a measure of the amount of each S oxidation state relative to total S content in samples.

2.4. Binding Affinity Experiments using Halides as Competitive Ligands

We took advantage of the strong complexation between methyl mercury and halides for the determination of the binding strength of methyl mercury to soil organic matter. Duplicates of homogenized 0.5 g freeze-dried organic soil (OS) sample from Svartberget were suspended in 30 ml solutions of either 0.01 M KBr, 0.01M Kl or 0.01 M KNO_3 in 50 ml polypropylene centrifuge tubes at 25 °C, pH (at equilibrium) was adjusted between 3.0 and 4.3 by an addition of sodium hydroxide. The suspensions were shaken for 24 h for soil adsorbed methyl mercury to reach equilibrium with halide and organic complexes in solution. We tested that equilibrium was reached by similar experiments extended to 96 h of shaking. These experiments yielded similar results as after 24 h (data not shown). At equilibrium methyl mercury in the solution phase of the KNO_3 suspension is 100% complexed by dissolved organic ligands released from the soil, whereas halide complexes (CH_3HgBr and CH_3HgI) also contribute significantly to the concentration of dissolved species in the KBr and KI suspensions. After centrifugation of suspensions for 15 min at 5,000 rpm, the supernatant was decanted and added 2 ml of 0.1 M $AgNO_3$ in order to precipitate free iodide or bromide ions as Ag complexes (to avoid interference during subsequent derivatization). The total concentration of methyl mercury in the aqueous phase was determined after extraction followed by *in situ* ethylation (derivatization), GC separation and microwave induced plasma atomic emission spectrometry detection in accordance to the method of Qian et al. (2000). Soil adsorbed methyl mercury was calculated as the difference between methyl mercury concentration in the moist soil samples prior to freeze drying, determined by the method of Qian et al. (2000), and total mercury concentrations in the aqueous phase after equilibration.

In order to calculate the concentration of CH_3Hg–halide complexes in the aqueous phase of the KBr and KI suspensions, the concentration of dissolved, organically complexed CH_3Hg was corrected for. This was done by a simple proportionality, based on the assumption that all dissolved CH_3Hg was organically complexed in the KNO_3 suspensions (Skyllberg et al., 2000). This assumption was proven valid by our results (see the Results and Discussion section). The ratio between organically complexed CH_3Hg in aqueous phase, CH_3Hg_{DOC}, and dissolved organic carbon (CH_3Hg_{DOC}/DOC), and the ratio between organically complexed Hg in soil (CH_3Hg_{SOC}) and soil organic carbon (CH_3Hg_{SOC}/SOC), were calculated in the KNO_3 suspensions. Provided that the quotient between the ratios CH_3Hg_{DOC}/DOC and CH_3Hg_{SOC}/SOC is not changed by addition of a strong complexation agent like bromide or iodide, CH_3Hg complexed by DOC in the potassium bromide or iodide suspensions $(CH_3Hg_{DOC})_{KBr/KI}$, can be calculated by the following equation:

$$(CH_3Hg_{DOC})_{KBr/KI} = [(DOC)(CH_3Hg_{SOC})/(SOC)]_{KBr/KI} \times [(SOC)(CH_3Hg_{DOC})/(DOC)(CH_3Hg_{SOC})]_{KNO3} \quad (1)$$

The amount of CH_3Hg_{DOC} was subtracted from the amount of total dissolved mercury in the halide suspensions to yield the amount of CH_3HgBr or CH_3HgI in the aqueous phase. The activity of free, noncomplexed methyl mercury $\{CH_3Hg^+\}$ in the aqueous phase of the suspensions was calculated using the speciation program MINTEQA2 (Allison and Brown, 1995) and stability constants for bromide (log $K_{CH3HgBr}$ = 6.62) and iodide complexes (log K_{CH3HgI} = 8.60) taken from Smith and Martell (1993).

The conditional constant for the reaction between methyl mercury and dissociated, reduced organic sulfur groups (RS^-) in soil organic matter

$$RS^- + CH_3Hg^+ = CH_3Hg\ SR \quad (2)$$

is calculated by Eqn. 3,

$$K_{CH_3HgSR} = [CH_3Hg\ SR]/([RS^-]\ \{CH_3Hg^+\}). \quad (3)$$

Square brackets [ ] designate concentrations in units mol g^{-1} and curly brackets { } denote activities in the aqueous phase calculated by the Davies equation (in MINTEQA2). Reduced organic S groups (Org-S_{RED}), determined by XANES, were taken to represent RSH, and the average dissociation constant of thiol (log K_{RSH} = 9.96; mercaptoacetic acid, Hilton et al., 1975) was used to calculate the concentration of dissociated ligand.

3. RESULTS AND DISCUSSION

3.1. Concentration of Reduced Organic Sulfur Functionalities (Org-S_{RED})

In Table 1 total concentrations of C, N, and S are given together with Org-S_{RED} determined by S XANES analysis. In Figure 1 XANES spectra for the three samples taken along the "hydrological transect" at Svartberget, and for the Norwegian fen peat, are shown. In Table 2 quantitative data for these four spectra, and for the FPOS sample, are given in form of four to six major electronic oxidation states, as determined by the linear relationship between white line maximum and formal oxidations states of S standard compounds with integer oxidation numbers (Waldo et al., 1991; Morra et al., 1997; Xia et al., 1998).

First it is noticed that none of the five samples analyzed contained any detectable amounts of inorganic sulfides, which would have given rise to a peak at lower energies than −0.5 eV, relative to elemental S (Huffman et al., 1991). Given the uncertainties of the method used to deconvolute the XANES spectrum into pseudocomponents (cf. Beauchemin et al., 2002), it cannot be completely ruled out that small quantities of inorganic sulfides were present in the samples. Most important, possible traces of inorganic sulfides would not have contributed significantly to the bonding of CH_3Hg(II), except possibly at the lowest CH_3Hg (II)/Org-S_{RED} ratio (0.01).

Overall the organic S species are distributed into two major groups: reduced S, at energies below approximately 2 eV relative to elemental S, and oxidized S at energies above approximately 6 eV. This bimodal pattern is in agreement with recent XANES determinations of humic substances (Morra et al., 1997; Xia et al., 1998; Hutchison et al., 2001; Szulczewski et al., 2001). Sulfur electronic oxidation states of 6.0, 5.0, and

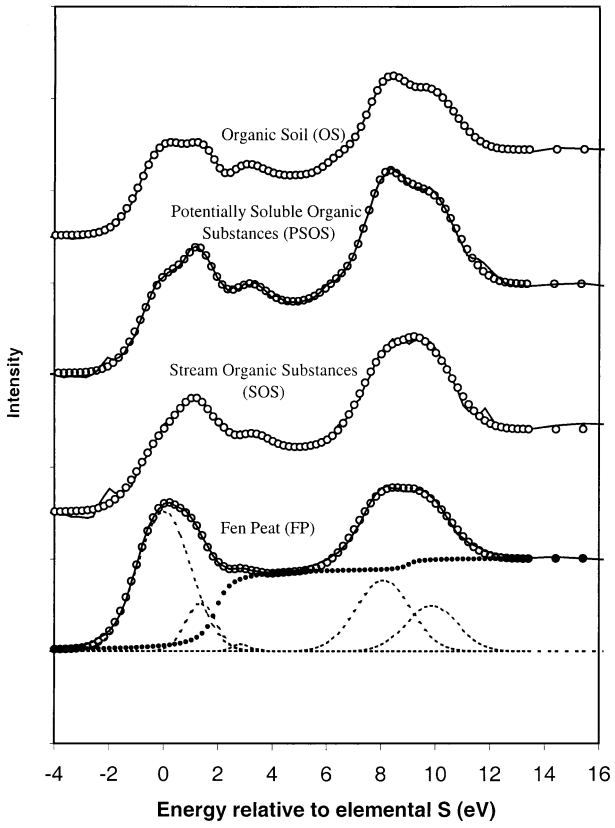

Fig. 1. Sulfur *K*-edge XANES spectra for samples OS, PSOS, SOS, and FP. The energy is normalized to the *K* edge of elemental S (2,472 eV). Solid lines represent experimental data and open circles represent least-squares-fitted spectra. Deconvolution of the FP experimental spectrum into pseudocompounds is shown at the bottom. Dashed and dotted lines represent Gaussian peaks for five different sulfur oxidation states and background, respectively. The energy position of each of these peaks is given in Table 2.

Table 2. Gaussian component peak parameters derived from least-square fitting of S *K*-edge XANES spectra (Fig. 1). Peak maximum energy is given in relation to elemental S (2472 eV). Relative abundance of S electronic oxidation state species is expressed as % of total S. Org-S_{RED} represents S with electronic oxidation state of 0.2.

Peak maximum energy eV	S electronic oxidation state*	Fraction† (% of S_{tot})
	Organic soil (OS)	
0.3	0.2	46.7
1.7	1.0	14.5
3.1	1.9	5.2
6.6	4.0	2.0
8.3	5.0	17.4
10.0	6.0	14.2
	Potentially soluble organic substances (PSOS)	
0.4	0.2	42.5
1.6	1.0	13.7
3.3	2.0	4.6
6.7	4.0	3.0
8.3	5.0	17.5
10.0	6.0	18.6
	Stream organic substances (SOS)	
0.4	0.2	39.0
1.6	0.9	18.4
3.5	2.1	3.4
8.3	5.0	18.7
10.0	6.0	20.6
	Fen peat (FP)	
0.4	0.2	64.0
1.6	0.9	10.6
3.5	2.1	0.8
8.3	5.0	15.9
10.0	6.0	8.6
	Fen peat organic substances (FPOS, not shown in Fig. 1)	
0.2	0.2	27.4
1.5	0.9	6.7
8.4	5.0	20.2
10.0	6.0	45.5

* Waldo et al (1991); Xia et al (1998).
† Estimated error is ± 5–10 % of given values.

4.0 correspond to sulfate-esters (and inorganic sulfate), sulfonates, and sulfoxides, respectively. Quantification and identification of S compounds in the reduced end of the spectrum is a slightly more delicate task. Because of this, Skyllberg et al. (2000) used the sum of S electronic oxidation states 0.2 and 1.0 as a conservative estimate of reduced organic S functional groups in model calculations.

The peak representing the most reduced organic S functional groups has an electronic oxidation state around 0.2. This peak likely corresponds to a sum of thiol (RSH), disulfane (RSSH), organic sulfide (RSR) and possibly organic disulfide (RSSR) functionalities (Waldo et al., 1991; Huffman et al., 1991; Xia et al., 1998). Sites included in this peak are in this study designated Org-S_{RED}. The relative concentration of these groups apparently decreases along the hydrological transect at Svartberget from 46.7% of total S in the organic soil to 39.0% in the stream (Table 2). The PSOS has an intermediate value (42.5%). For the most oxidized S (sulfate esters), with an electronic and formal oxidation state of 6.0, the trend is the opposite with the highest relative concentration in the stream, followed by the PSOS. These differences in S speciation along the hydrological transect may not be significant given the fact that the error is estimated to be ±5%–10% of the reported value.

Hundal et al. (2000) reported the hydrophobic fraction of fulvic acids to have substantially higher relative concentrations of reduced S (electronic oxidation states below 2) than the hydrophilic fraction. Hydrophobic organic substances are known to preferentially adsorb in soils (e.g., Kaiser et al., 1996). Thus, one explanation for the decrease of Org-S_{RED} from the organic soil to stream at Svartberget may be a corresponding decrease in the hydrophobic organic fraction due to soil adsorption. Another possible explanation is that the extraction of the organic soil and treatment of the stream organics resulted in an oxidation of some highly reduced organic S, leading to a higher relative concentration of oxidized S in PSOS. Against this speaks the finding by Hutchison et al. (2001) that reduced organic S (determined by XANES) shows a very strong resistance to oxidation during exposure of humic acid to O_2 for up to 44 h duration at pH between 3.5 and 11.4.

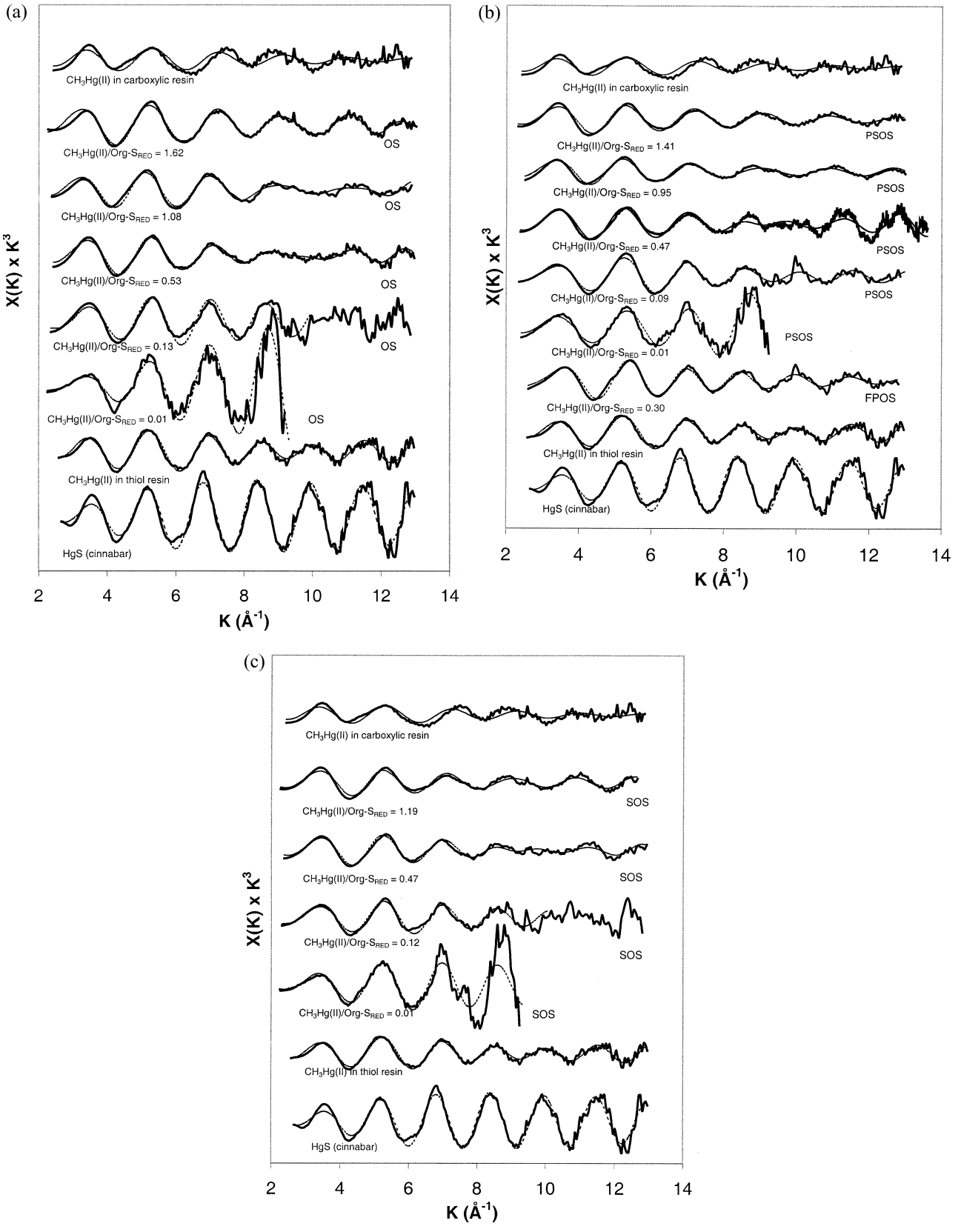
(a)
CH3Hg(II) in carboxylic resin
CH3Hg(II)/Org-SRED = 1.62
OS
CH3Hg(II)/Org-SRED = 1.08
OS
CH3Hg(II)/Org-SRED = 0.53
OS
CH3Hg(II)/Org-SRED = 0.13
OS
CH3Hg(II)/Org-SRED = 0.01
OS
CH3Hg(II) in thiol resin
HgS (cinnabar)
X(K) x K3
2 4 6 8 10 12 14
K (Å-1)
(b)
CH3Hg(II) in carboxylic resin
CH3Hg(II)/Org-SRED = 1.41
PSOS
CH3Hg(II)/Org-SRED = 0.95
PSOS
CH3Hg(II)/Org-SRED = 0.47
PSOS
CH3Hg(II)/Org-SRED = 0.09
PSOS
CH3Hg(II)/Org-SRED = 0.01
PSOS
CH3Hg(II)/Org-SRED = 0.30
FPOS
CH3Hg(II) in thiol resin
HgS (cinnabar)
X(K) x K3
2 4 6 8 10 12 14
K (Å-1)
(c)
CH3Hg(II) in carboxylic resin
CH3Hg(II)/Org-SRED = 1.19
SOS
CH3Hg(II)/Org-SRED = 0.47
SOS
CH3Hg(II)/Org-SRED = 0.12
SOS
CH3Hg(II)/Org-SRED = 0.01
SOS
CH3Hg(II) in thiol resin
HgS (cinnabar)
X(K) x K3
2 4 6 8 10 12 14
K (Å-1)

It should be noted that the organic soil sampled was above the ground water table and was oxidized in that meaning that it was fully exposed to air and aerated soil water in its natural environment for weeks prior to sampling.

The FP sample was selected for this study because of its high concentration of total S. The XANES analyses showed that 64.0% of total S was made up by Org-S_{RED} in the FP soil, as compared to 27.4% in the organic extract of the FP soil (FPOS), Table 2. This large difference is mainly explained by a release of sulfate ions from the FP soil during extraction. Since the extract was not dialysed prior to freeze drying, even relatively small quantities of sulfate released from the soil results in a high relative concentration of sulfate in the freeze-dried sample. The source of sulfate may be from traces of sulfate salts (soil solution was slightly undersaturated in relation to gypsum) or possibly by an oxidation of reduced organic S groups in the soil during extraction. As a consequence of this, S_{tot} was higher and Org-C and N_{tot} was substantially lower in FPOS than in FP (Table 1). Because of dilution by salts, the Org-S_{RED}/Org-C ratio is a better estimate of the density of reduced organic S in organic substances. This ratio was higher in the extract (PSOS) than in the soil (OS) along the hydrological transect, and the other way around for FPOS–FP.

3.2. CH_3Hg–organic Matter Bonding as Determined by Hg L_{III} Edge EXAFS

In Figures 2a–c the k^3-weighted EXAFS spectra (chi data) are presented at different CH_3Hg (II)/Org-S_{RED} ratios for the soil and stream samples, as well as for three reference compounds. Note that the noise in the spectra increases with decreasing methyl mercury concentration, i.e., with decreasing CH_3Hg (II)/Org-S_{RED} ratio. For the samples with lowest concentrations of methyl mercury [CH_3Hg (II)/Org-S_{RED} = 0.01], the *k*-space data extend only to 9.3 Å. Beyond 9.3 Å, the absorption of selenium present in the samples (selenium *K* edge at 12,658 eV) created a substantial disturbance in the Hg L_{III} EXAFS spectra. The phase of the oscillations in the *k* space corresponds mainly to interatomic distances (*R*) between Hg and coordinating atoms, whereas the type of atoms and their coordination numbers (*N*) and bonding disorder (represented by the Debye–Waller factor σ^2 in data fitting analysis) determine the amplitude. Fitting results for the model compounds are shown in Table 3 and for the organic soil and stream samples in Table 4.

The Fourier transformed EXAFS data (*R* space data), expressed as the radial structure function (RSF), are illustrated in Figure 3a–c. The intensity variations below 1 Å are partly due to residual background noise in the *k*-space data. The major peaks within the range of 1.5 to 2 Å in the RSF curves reflect the average, relative distances (not corrected for phase shift) to atoms in the first coordination shell of Hg.

The reference compound cinnabar (red HgS) shows a distinct peak at 1.98 Å in the RSF, reflecting the backscattering from two sulfur atoms at distance of 2.37 Å (Table 3). The binding distance was obtained from fitting when the coordination number was constrained close to the known value of 2.0. The distance of 2.37 Å is in agreement with earlier determinations using various empirical and theoretical methods (Tossell, 2001). The peak at 1.98 Å in the RSF is also apparent in the thiol-resin sample, reflecting the Hg–SR (R = carbon chain) bond in the CH_3Hg–SR resin. The smaller peak at approximately 1.55 Å in the RSF reflects the backscattering from C within the methyl mercury molecule, at a distance of 2.04 Å from Hg (Table 3). The Hg–S bond length determined (2.33 Å) is within the range from 2.30 to 2.38 Å reported for two-coordinated Hg with S in sulfur containing amino acids and metallothionines (Taylor et al., 1975; Klemens et al., 1989; Raybuck et al., 1990; Jiang et al., 1994; Lobana et al., 1997), as well as in a humic acids (Xia et al., 1999; Hesterberg et al., 2001). This distance is also in fair agreement with the bond length/bond strength relationship reported by Brown and Altermatt (1985), suggesting a bond length of 2.31 Å. An amplitude reduction factor (S_0^2) of 0.93 was obtained from the best fit of the thiol resin. This value was used when fitting data of the OS, PSOS, SOS, and FPOS samples, since the thiol resin is supposed to be the most relevant model compound for the binding of methyl mercury in organic matter. Also in cinnabar, where Hg is two coordinated with S, a fairly similar amplitude reduction factor (0.90) was determined.

With EXAFS, O and N atoms are difficult to separate from each other, as well as from C. All these atoms show a peak in the range 1.55–1.65 Å in the RSF. Since there are no O or N containing ligands in the thiol resin, the minor peak in this sample with certainty represents C. In the carboxylic resin a mixture of Hg–C (within the methyl mercury molecule) and Hg–O bonds (the CH_3Hg–OOR association) give rise to a broad peak centered at approximately 1.6 Å. The carboxylic resin data were best fitted by Hg coordinated to one C atom at a distance of 2.03 Å and to one O atom at a distance of 2.09 Å (Table 3). These distances are within ranges for Hg–C and Hg–O bond lengths reported for well-defined organic molecules. The distance of the Hg–C bond has been reported to be in the range of 2.01–2.08 Å by Kashiwabara et al. (1973), Barone et al. (1995), and Lobana et al. (1997) for two-coordinated Hg in methyl mercury halides, as well as in Hg $(CN)_2$. In

Fig. 2. (a) Stacked, normalized, k^3-weighted EXAFS spectra for model compounds and for methyl mercury bound to the organic soil (OS) at five different CH_3Hg (II)/Org-S_{RED} molar ratios. Experimental spectra (solid lines) are overlaid with spectra derived from fitting parameters (dashed lines) in Table 3 (model compounds) and in Table 4 (OS). (b) Stacked, normalized, k^3-weighted EXAFS spectra for model compounds and for methyl mercury bound to the extracted potentially soluble organic substances from the soil (PSOS) and from the fen peat (FPOS). For PSOS samples, spectra are shown at five different CH_3Hg (II) / Org-S_{RED} molar ratios. The spectrum for PSOS sample CH_3Hg (II)/Org-S_{RED} = 0.47 represents a merge of 120 scans, each collected during 40 seconds with a quick-scan procedure. Experimental spectra (solid lines) are overlaid with spectra derived from fitting parameters (dashed lines) presented in Table 3 (model compounds) and in Table 4 (PSOS and FPOS). (c) Stacked, normalized, k^3-weighted EXAFS spectra for model compounds and for methyl mercury bound to the stream organic substances (SOS) at four different CH_3Hg (II)/Org-S_{RED} molar ratios. Experimental spectra (solid lines) are overlaid with spectra derived from fitting parameters (dashed lines) presented in Table 3 (model compounds) and in Table 4 (SOS).

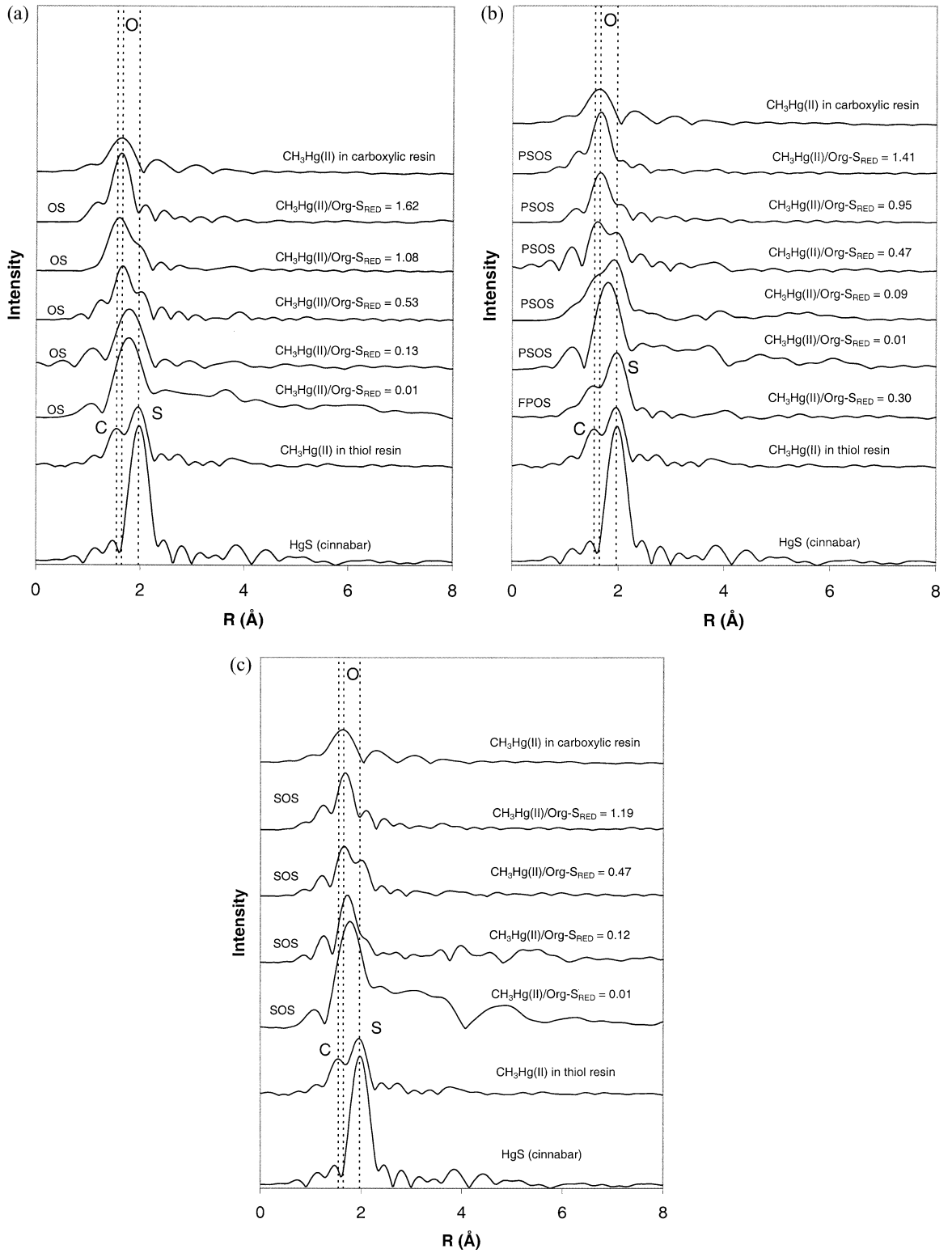

Fig. 3. (a) Stacked, Fourier transformed EXAFS spectra for model compounds and for methyl mercury bound to organic soil (OS). The CH_3Hg (II)/Org-S_{RED} molar ratio is given for each sample. Spectra are not corrected for phase shift. (b) Stacked, Fourier transformed EXAFS spectra for model compounds and for methyl mercury bound to extracted potentially soluble organic substances from the soil (PSOS) and from the fen peat (FPOS). The CH_3Hg (II)/Org-S_{RED} molar ratio is given for each sample. Spectra are not corrected for phase shift. (c) Stacked, Fourier transformed EXAFS spectra for model compounds and for methyl mercury bound to stream organic substances (SOS). The CH_3Hg (II)/Org-S_{RED} molar ratio is given for each sample. Spectra are not corrected for phase shift.

Table 3. Hg L_{III} edge EXAFS *k*-space fitting results for methyl mercury (carboxyl and thiol resins) and mercury (cinnabar) model compounds. The coordination number (N) and the first coordination shell bond length (R) have a precision of approximately ± 15% and ± 0.02 Å, respectively. The $\Delta\sigma^2$ is the Debye–Waller factor. Difference in edge energy is represented by ΔE^0. For cinnabar the coordination number was constrained close to the theoretical number of 2. The determined amplitude reduction factor S^2_0 was 0.90 for cinnabar and the carboxylic resin and 0.93 for the thiol resin. Note that Hg–O bonding was not distinguished from Hg–N bonding.

Model compound	First-shell bond	N	R (Å)	$\Delta\sigma^2$ (Å^2)	ΔE^0(eV)
CH_3Hg (II) bound to carboxylic resin	Hg–C	1.10	2.03	0.005	3.0
	Hg–O	0.90	2.09	0.007	
CH_3Hg (II) bound to thiol resin	Hg–C	1.00	2.04	0.002	0.9
	Hg–S	1.15	2.33	0.004	
Cinnabar (red HgS)	Hg–S	1.99	2.37	0.002	4.2

a review article, Holloway and Melnik (1995) reported a Hg–O bond distance range of 2.07–2.09 Å for two-coordinated Hg in organomercurials bound to organic compounds. They reported the Hg–N distance in similar compounds to vary between 2.05 and 2.16 Å. Thus, Hg–C, Hg–O, and Hg–N bonds for two-coordinated Hg in organomercurials bound to organic compounds are similar in distance, but there is a tendency for slightly longer bonds with increasing atomic radius (C < O < N).

The Fourier transformed data for the Norwegian fen peat [CH_3Hg (II)/Org-S_{RED} = 0.30] look very similar to those for the thiol resin, with both a smaller C peak at 1.55 Å and a bigger S peak at 1.95 Å in the RSF (Fig. 3b). A linear model, with one C atom (N = 1.2) at 2.03 Å distance (the methyl group) and one S atom (N = 1.2) at 2.33 Å distance from Hg (Table 4), showed the best fit to this sample. An introduction of O and/or N atoms in the model (applying a model with floating coordination numbers for C + S + O/N atoms) gave worse fits. Reasonable fits were only obtained when the coordination number for O and/or N was close to zero. Thus, in the Norwegian fen peat CH_3Hg^+ formed a mono-dentate bond with reduced S groups.

The RSF data for the samples taken along the hydrological transect (OS, PSOS, and SOS) show a very similar pattern with increasing CH_3Hg (II)/Org-S_{RED} molar ratio (Figs. 3a, 3b, and 3c). At the two lowest ratios (0.01 and 0.09–0.13), one broad peak is centered at 1.75–1.80 Å. The lack of features in these peaks is partly due to noise in the data at low methyl mercury concentrations (100–1000 mg kg^{-1}) and partly due to the limited *k* space range for these samples (because of strong interference by selenium absorption above 9.3 Å). The quality of data for the PSOS sample with a ratio of 0.09 was slightly better. The Hg–C bond is reflected by the shoulder at 1.55 Å and the Hg–S bond is reflected by a major peak at 1.90 Å in the RSF. Fitting in *k* space show that the broad peak at 1.75–1.80 Å, for the two lowermost CH_3Hg (II)/Org-S_{RED} molar ratios, represents a mixture of one Hg–C and one Hg–S bond at 2.03–2.06 Å and 2.31–2.32 Å, respectively (Table 4). On average 1.16 ± 0.05 (SD) C atoms and 1.17 ± 0.06 (SD) S atoms were found in the first coordination shell of Hg for the OS, PSOS, and SOS samples with the two lowermost CH_3Hg (II) / Org-S_{RED} ratios (0.01 and 0.09–0.13). The average distances of Hg–C and Hg–S bonds were 2.05 ± 0.01 Å and 2.31 ± 0.01 Å, respectively. These distances are very similar to the distances for Hg–C and Hg–S bonds in the thiol-resin model compound (Table 3), as well as for similar bonds reported in the literature (see above). As for the FPOS sample, reasonable fits with a model consisting of floating coordination numbers of C, S, and O/N atoms were only obtained when the coordination number of O/N was close to zero.

At an intermediate CH_3Hg (II) / Org-S_{RED} ratio from 0.47 to 0.53 for the OS, PSOS, and SOS samples, one larger peak shows up at 1.6 Å in the RSF, representing a mixture of bonds to C and O/N atoms, and a shoulder at 1.95–2.0 Å, representing a Hg–S bond. At even higher CH_3Hg (II)/Org-S_{RED} ratios

Table 4. Hg L_{III} edge EXAFS *k*-space fitting results for methyl mercury bound to OS, PSOS, SOS, and FPOS at different CH_3Hg/Org-S_{RED} ratios and pH 3.8–4.0. The amplitude reduction factor S_0^2 was fixed at 0.93. The edge energy ΔE^0 was allowed to vary, but constrained to the same value for all atoms in the first coordination shell. N is the coordination number (±15%), R is the first-shell bond length (±0.02 Å), and $\Delta\sigma^2$ is the Debye–Waller factor. Hg–O bonding was not distinguished from Hg–N.

Sample or standard	CH_3Hg (II)/ Org-S_{RED}	First-shell bond	N	R (Å)	$\Delta\sigma^2$ (Å^2)	ΔE^0 (eV)
Organic soil (OS)	1.62	Hg–C	1.18	2.02	0.001	2.0
		Hg–O	1.10	2.09	0.001	
		Hg–S	0.27	2.37	0.008	
	1.08	Hg–C	1.00	2.02	0.001	−0.9
		Hg–O	0.88	2.10	0.002	
		Hg–S	0.66	2.33	0.008	
	0.53	Hg–C	1.10	2.03	0.001	3.4
		Hg–O	0.54	2.11	0.001	
		Hg–S	0.83	2.35	0.008	
	0.13	Hg–C	1.20	2.06	0.008	1.3
		Hg–S	1.05	2.31	0.003	
	0.01	Hg–C	1.06	2.06	0.001	−0.8
		Hg–S	1.20	2.31	0.001	
Potentially soluble organic substances (PSOS)	1.41	Hg–C	1.10	2.02	0.001	4.2
		Hg–O	1.10	2.09	0.002	
		Hg–S	0.30	2.36	0.009	
	0.95	Hg–C	1.15	2.04	0.003	2.5
		Hg–O	0.72	2.09	0.003	
		Hg–S	0.53	2.37	0.009	
	0.47	Hg–C	1.10	2.04	0.002	4.2
		Hg–O	0.56	2.08	0.001	
		Hg–S	0.65	2.37	0.002	
	0.09	Hg–C	1.20	2.04	0.004	−0.3
		Hg–S	1.20	2.32	0.005	
	0.01	Hg–C	1.12	2.06	0.007	1.5
		Hg–S	1.19	2.31	0.001	
Stream organic substances (SOS)	1.19	Hg–C	1.18	2.02	0.003	3.0
		Hg–O	1.09	2.09	0.002	
		Hg–S	0.24	2.40	0.003	
	0.47	Hg–C	1.09	2.02	0.002	3.1
		Hg–O	0.60	2.09	0.001	
		Hg–S	0.85	2.36	0.005	
	0.12	Hg–C	1.20	2.03	0.006	−0.2
		Hg–S	1.14	2.31	0.004	
	0.01	Hg–C	1.15	2.05	0.002	−0.8
		Hg–S	1.19	2.31	0.001	
Fen peat organic substances (FPOS)	0.30	Hg–C	1.20	2.03	0.006	3.7
		Hg–S	1.20	2.33	0.005	

Table 5. Fraction of high affinity Org-S_{RED} sites taking part in the bonding of CH_3Hg in OS, PSOS, and SOS, as calculated by Eq. 4.

OS		PSOS		SOS	
CH_3Hg (II)/ Org-S_{RED} molar ratio	High affinity fraction of Org-S_{RED}	CH_3Hg (II)/ Org-S_{RED} molar ratio	High affinity fraction of Org-S_{RED}	CH_3Hg (II)/ Org-S_{RED} molar ratio	High affinity fraction of Org-S_{RED}
0.53	0.33	0.47	0.27	0.47	0.27
1.08	0.46	0.95	0.40	1.19	0.22
1.62	0.32	1.41	0.30		
Average	0.37 ± 0.08	Average	0.32 ± 0.07	Average	0.24 ± 0.04

(0.95–1.62) the peak at 1.6 Å predominates and the shoulder at 1.95–2.0 Å decreases with increasing ratio. This overall pattern reflects a gradual saturation of reduced S sites by CH_3Hg^+ at increasing CH_3Hg (II)/Org-S_{RED} ratio. When the high affinity reduced S sites are saturated, CH_3Hg^+ gradually occupies weaker binding sites such as O- and/or N-containing functional groups. For OS, PSOS, and SOS samples with a CH_3Hg (II) / Org-S_{RED} ratio from 0.47 to 1.62 the average distances of Hg–C, Hg–O/N, and Hg–S bonds were 2.03 ± 0.01 Å, 2.09 ± 0.01 Å, and 2.36 ± 0.02 Å, respectively. To ensure that fitting results for samples with the lowest CH_3Hg (II)/Org-S_{RED} ratio were not caused by the limited *k* range, also intermediate and high CH_3Hg (II)/Org-S_{RED} ratio samples were fitted below 9.3 Å. No substantial changes in fitting parameters were observed.

It is a common observation from EXAFS studies of environmental samples that the coordination number shows an uncertainty on the order of 15–30 % (e.g., Hesterberg et al., 2001). In this study, on average 1.14 ± 0.06 (SD) C atoms were found in the first coordination shell of Hg for our 15 soil and organic samples listed in Table 3. Very similar coordination numbers for C and S atoms in the samples with the two lowermost CH_3Hg (II)/Org-S_{RED} ratios (1.16 and 1.17, respectively), even though they are slightly above unity, strongly suggests that the methyl mercury molecule is kept intact and adsorbed to one S atom in soil and stream organic matter. This conclusion is reasonable since the covalent Hg–C bond in methyl mercury is relatively strong and was shown to be stable in the thiol-resin sample.

Despite the fact that we at beamline ID 26, ESRF, were able to study the binding of methyl mercury in soil and stream organic samples at concentration as low as 100 mg CH_3Hg(II) per kg soil, this concentration is still much higher than in most soil and stream samples. However, since 100 mg CH_3Hg (II) per kg soil corresponds to a CH_3Hg (II)/Org-S_{RED} ratio of 0.01, it is reasonable to assume that CH_3Hg^+ would bind to reduced S groups in soil also at lower ratios.

The addition of A1 to PSOS and SOS will likely have no effect on EXAFS results. Because of the very weak bonding of Al cations [Al^{3+}, $Al(OH)_n^{3-n}$, hard Lewis acids] to reduced S groups (and N groups, soft Lewis bases), Al will not compete with CH_3Hg^+ for these groups. In the case when RSH groups are saturated, there might be a competition between CH_3Hg and Al for different types of oxygen groups. Such a competition will, however, not be possible to trace in the EXAFS spectra since there will always be oxygen sites enough for both Al and CH_3Hg.

3.3. Quantification of CH_3Hg-Bonding Organic S Sites by use of Hg EXAFS

If it is assumed that certain reduced S groups possess the strongest binding sites for CH_3Hg^+ in soil and stream organic matter, as suggested by our EXAFS observations, and that these sites will be saturated before weaker O/N containing sites may take part in the bonding, our EXAFS results can be used for further chemical speciation of Org-S_{RED} determined by XANES. By use of Eqn. 4, where *N* is the coordination number for the Hg association to reduced organic S and O/N atoms taken from EXAFS results in Table 3, the fraction of Org-S_{RED} consisting of high affinity sites (stronger than O and N) is calculated:

$$\text{Fraction of Org-}S_{RED}\text{ high affinity sites} = N_{Sulfur} / (N_{Sulfur} + N_{Oxygen/Nitrogen}) \times CH_3Hg\text{ (II)/ Org-}S_{RED}. \quad (4)$$

This calculation shows that on average 37% of Org-S_{RED} in the organic soil, 32% in the potentially soluble organic substances from the soil, and 24% of Org-S_{RED} in the stream organic matter represents high affinity CH_3Hg-binding groups (Table 5). If the fraction of CH_3Hg-binding reduced organic S groups are expressed in relation to total S, 17% is found in OS, 14% in PSOS, and only 9% in SOS. Even though our samples are to few for general conclusions, it is clear that the solid phase of organic matter in the soil investigated possessed both a higher relative and absolute concentration of high affinity S sites, as compared to dissolved organic substances in both soil and stream. This decrease in high affinity S site density in organic substances along the hydrological transect from soil to stream is interesting and should be investigated further in different types of watersheds.

Although CH_3Hg^+ and Al cations do not compete for reduced S sites, it cannot be completely excluded that the relatively strong affinity of Al for oxygen sites could have an effect of forcing some CH_3Hg to "weaker S sites," as compared to a case without Al. If so, the observation that PSOS and SOS (both added Al) had a lower portion of high affinity reduced organic S groups than OS (not added Al, but with natural content of Al) would be even more pronounced.

Thiol groups likely are the main contributors to the high affinity S groups calculated by Eqn. 4. Even if it cannot be excluded that also RSSH, RSR, and RSSR functionalities may contribute to strong bonding of CH_3Hg^+ in natural organic matter, our results may be taken as an indication that on the order of 25%–40% of the most reduced organic S functionalities, as determined by XANES, are thiols.

3.4. Binding Affinity of Methyl Mercury in Organic Soil

Binding affinity data from the organic soil (OS) were evaluated using the model described by Eqn. 3. The model was chosen because it is commonly used to described the binding of CH_3Hg (II) to well-defined organic substances (formation constants, K_1), and because our combined XANES + EXAFS data strongly suggest that CH_3Hg (II) is associated with thiol groups through a mono-dentate bond in the OS sample. Equation 3 was used to calculate an average, conditional complexation constant ($K_{CH3HgSR}$) based on data for the concentration of organically complexed CH_3Hg (II) [CH_3HgSR], the concentration of free, dissociated thiol groups [RS^-], and the activity of free [CH_3Hg^+].

Conditional stability constants (log K_{CH_3HgSR}), determined after 24 h of equilibration at 25°C and an ionic strength of 0.01 M, showed a slight pH dependence increasing from 16.3 ± 0.1 (n = 3) at pH 3.0, 16.5 ± 0.1 (n = 3) at pH 3.4–3.8 to 16.7 ± 0.1 (n = 3) at pH 4.3. The values were independent on whether Br^- (16.3 ± 0.1 at pH 3.8) or I^- (16.5 ± 0.1 at pH 3.8) was used as competing ligand, or if the equilibrium time was extended to 96 h. These constants are all based on the assumption that Org-S_{RED} can be taken as an estimate of the CH_3Hg^+ binding groups (RSH in the model) in the soil. If instead only the high affinity fraction of Org-S_{RED}, as determined by Eqn. 4 and given in Table 5, is used as an estimate of RSH groups the above given constants will increase by approximately 0.4 log units from the range 16.3–16.7 to 16.7–17.1.

Our determined conditional constants compare favorably with identically defined stability constants (log K_1) for the binding of methyl mercury to thiol groups in 2-amino-3-mercapto-propanoic acid (log K_1 = 16.7), 2-amino-4-mercaptobutanoic acid (log K_1 = 16.4), DL-2-amino-3-mercapto-3-methylbutanoic acid (log K_1 = 16.9) and N-acetyl-penicillamine (log K_1 = 16.8), Reid and Rabenstein (1981). Although possible electrostatic effects from soil surface charges and the heterogeneity of soil organic substances were not considered in our model, the similar magnitude of our conditional constants to tabulated stability constants strongly indicates that thiol groups are involved in the binding of CH_3Hg (II) at a CH_3Hg (II)/ Org-S_{RED} ratio of approximately 10^{-7}. Based on our determined conditional formation constants, the concentration of free CH_3Hg^+ and inorganic complexes (CH_3HgOH) were on the order of 10^{-17} M in our KNO_3 batch experiments, as compared to 10^{-12} M for dissolved CH_3Hg–DOC complexes. Thus, the assumption that the concentration of free CH_3Hg^+ did not contribute significantly to the total concentration of dissolved CH_3Hg in our KNO_3 experiments is accurate.

Under oxidized conditions in fresh water systems and in soils, chloro complexes may contribute to the complexation of methyl mercury in the aqueous phase. However, based on our conditional stability constants, the bonding of methyl mercury to reduced organic S groups is strong enough to keep the concentration of chloro -complexes as low as 10^{-17} to 10^{-16} M in typical boreal forest soils and streams.

Hintelmann et al. (1997) used the Scatchard model to determine the binding affinity of methyl mercury to aqueous humic and fulvic acids. The conditional stability constants calculated as log K = log ([CH_3HgHS] / ([CH_3Hg^+][HS])), where HS is the concentration of humic or fulvic acid, were 12.15–13.07 for a weak site and 13.02–14.56 for a strong site at pH 7.0. Calculated in a similar way, using Org-S_{RED} as [HS], our data give constants on the order of 14.5 at pH 7.0. Thus, the conclusion drawn by Hintelmann and co-workers that S groups are involved in the binding of CH_3Hg (II) to humic and fulvic acids is further supported by our study.

4. CONCLUSIONS

Based on results from combined S K-edge XANES + Hg L_{III}-edge EXAFS studies, and binding affinity studies, we conclude that CH_3Hg (II) preferentially forms complexes with reduced organic S groups in both soil and stream organic substances. If it is assumed that RSH, and possibly RSSH groups, associate strongly with CH_3Hg(II), whereas RSSR and RSR groups do not take part in the complexation, our results suggest that approximately 17% of total organic S in the organic soil consisted of RSH (+ RSSH) functionalities. Corresponding figures for potentially soluble organic substances from the soil and for stream organic substances were 14% and 9%, respectively. EXAFS data showed that O or N containing functional groups gradually take part in the binding only when reduced organic S sites are saturated by CH_3Hg^+. Conditional stability constants determined from binding affinity studies, using halides as competitors for natural organic ligands, compared favorably with tabulated constants for well-defined organic substances in which CH_3Hg^+ is complexed by thiol groups. Since in most soils reduced organic S groups are in large excess compared to methyl mercury, or even total mercury, we conclude that O or N groups do not take part in the binding of methyl mercury, except in severely contaminated soils.

Acknowledgments—The XANES experiments were conducted at beamline X19A at the National Synchrotron Light Source (NSLS), NY, USA. The EXAFS experiments were conducted at beamline X11A, NSLS and at beamline ID26 at the European Synchrotron Radiation Facility, Grenoble, France. We thank Soh-Joung Yoon at the Department of Soil Science, University of Wisconsin for assistance at NSLS. Lisa Miller and her staff at NSLS and the staff at ESRF are gratefully acknowledged. The Swedish Natural Science Research Council and CMF, Umea provided funding for this project.

Associate editor: D. L. Sparks

REFERENCES

Adams M.A. and Byrne L.T. (1989) ^{31}P-NMR analysis of phosphorus compounds in extracts of surface soils from selected karri (*Eucalyptus diversicolor* F. Muell) forests. *Soil Biol. Biochem* **21,** 523–528.

Allison J. D., Brown D. S. (1995) In *Chemical Equilibrium and Reaction Models* (ed. P. H. Loeppert), pp. 241–252, SSSA.

Barone V., Bencini A., Federico T., and Uytterhoeven M. G. (1995) Theoretical study of the electronic structure and of the mercury-carbon bonding of methylmercury(II) compounds. *J. Phys. Chem.* **99,** 12743–12750.

Beauchemin S., Hesterberg D., and Beauchemin M. (2002) Principal component analysis approach for modeling sulfur K-XANES spectra of humic acids. *Soil Sci. Soc. Am. J.* **66,** 83–91.

Bishop K.H. (1991) Episodic increases in stream acidity, catchment flow pathways and hydrograph separation. Ph.D. thesis. University of Cambridge.

Brown I. D. and Altermatt D. (1985) Bond-valence parameters obtained from a systematic analysis of the inorganic crystal structure database. *Acta Crystallogr* **B41,** 244–247.

Gauthier C., Solé V.A., Signorato R., Goulon J., and Moguiline E. (1999) The ESRF beamline ID26: X-ray absorption on ultra dilute sample. *J. Synchrotron Radiat.* **6,** 164–166.

Hesterberg D., Chou J. W., Hutchison K. J., and Sayers D. E. (2001) Bonding of Hg(II) to reduced organic sulfur in humic acid as affected by S/Hg ratio. *Environ. Sci. Technol.* **35,** 2741–2745.

Hintelmann H., Welbourn P.M., and Evans R. D. (1997) Measurement of complexation of methylmercury(II) compounds by freshwater humic substances using equilibrium dialysis. *Environ. Sci. Technol.* **31,** 489–495.

Hilton B. D., Man M., Hsi E., and Bryant R. G. (1975) NMR studies of mercury-halogen equilibria. *J. Inorg. Nucl. Chem.* **37,** 1073–1077.

Holloway C. E. and Melnik M. (1995) Mercury organometallic compounds—classification and analysis of crystallographic and structural data. *J. Organometal. Chem.* **495,** 1–31.

Hudson R. J., Gherini M. S. A., Watras C. J., and Porcella D. B. (1994) Modeling the biogeochemical cycle of mercury in lakes: the mercury cycling model (MCM) and its application to the MTL study lakes. In *Mercury Pollution Integration and Synthesis* (ed. C. J. Watras et al.). Lewis Publishers. CRC Press.

Huffman G. P., Mitra S., Huggins F. E., Shah N., Vaidya S., and Lu F. L. (1991) Quantitative-analysis of all major forms of sulfur in coal by x-ray absorption fine-structure spectroscopy. *Energ. Fuel.* **5,** 574–581.

Hundal L.S., Carmo A. M., Bleam W. F., and Thompson M. L. (2000) Sulfur in biosolids-derived fulvic acid: characterization by XANES spectroscopy and selective dissolution approaches. *Environ. Sci. Technol.* **34,** 5184–5188.

Hurley J., Benoit J., Babiarz C., Shafer M., Andren A., Sullivan J., Hammond R., and Webb D. (1995) Influences of watershed characteristics on mercury levels in Wisconsin rivers. *Environ. Sci. Technol.* **29,** 1867–1875.

Hutchison K. J., Hesterberg D., and Chou J. W. (2001) Stability of reduced organic sulfur in humic acid as affected by aeration and pH. *Soil Sci. Soc. Am. J.* **65,** 704–709.

Håkansson L. (1996) A simple model to predict the duration of the mercury problem in Sweden. *Ecol. Modell.* **93,** 251–262.

Jiang D. T., Heald S. M., Sham T. K., and Stillman M. J. (1994) Structures of the cadmium, mercury, and zinc thiolate clusters in metallothionein: XAFS study of Zn_7-MT, Cd_7-MT, Hg_7-MT and Hg_{18}-MT formed from rabbit liver metallothionein 2. *J. Am. Chem. Soc.* **116,** 11004–11013.

Kaiser K., Guggenberger G., and Zech W. (1996) Sorption of DOM and DOM fractions to forest soils.. *Geoderma* **74,** 281–303.

Kashiwabara K., Konaka S., Iijima T., and Kimura N. M. (1973) Electron diffraction study of dimethylmercury. *Bull. Chem. Soc. Jpn.* **46,** 407–409.

Klemens A. S., McMillin D. R., Tsang H., and Penner-Hahn J. E. (1989) Structure characterization of mercury-substituted copper proteins. Results from X-ray absorption spectroscopy. *J. Am. Chem. Soc.* **111,** 6398–6402.

Lobana T. S., Sanchez A., Casas J. S., Castineiras A., Sordo J., Garcia-Tasende M. S., and Vazquez-Lopez E. M. (1997) Symmetrisation, isomerism and structural studies on novel phenylmercury (II) thiosemicarbazonates: correlation of the energy barrier to rotation of the amino group with the bonding parameters of the thioamide group. *J. Chem. Soc., Dalton Trans.* **22,** 4289–4299.

Lytle F. W., Greegor R. B., Sandsrom D. R., Marques E. C., Wong J., Spiro C. L. , Huffman G. P., and Huggins F. E. (1984) Measurement of soft X-ray absorption spectra with a fluorescent ion chamber detector. *Nucl. Instrum. Methods Phys. Res.* **226,** 542–548.

Miller S. M., Moore M., Massey V., Williams C. H., Distefano M., Ballou D., and Walsh C. T. (1989) Evidence for the participation of Cys_{558} and Cys_{559} at the active site of mercuric reductase. *Biochemistry* **28,** 1194–1205.

Moore M. J., Distefano M.D., Zydowsky L.D., Cummings R. T., and Walsh C. T. (1990) Organomercurial lyase and mercuric ion reductase: nature's mercury detoxification catalysts. *Acc. Chem. Res.* **23,** 301–308.

Morra M. J., Fendorf S. E., and Brown P.D. (1997) Speciation of sulfur in humic and fulvic acids using X-ray absorption near-edge structure (XANES) spectroscopy. *Geochim. Cosmochim. Acta.* **61,** 683–688.

Morrison K. and Therien N. (1994) Mercury release and transformation from flooded vegetation and soils: experimental evaluation and simulation modeling. In *Mercury Pollution—Integration and Synthesis* (ed. C.J. Watras and J. W. Huckabee), pp. 355–365. Lewis Publishers, CRC Press.

Porcella D., Huckabee J., and Wheatley B. (1995) Mercury as a global pollutant. *Proceedings of the Third International Conference Held in Whistler, British Columbia, July 10–14, 1994.* Kluwer Academic Publishers.

Qian J., Skyllberg U., Tu Q., Bleam W. F., and Frech W. (2000) Efficiency of solvent extraction methods for the determination of methyl mercury in forest soils. *Fresenius J. Anal. Chem.* **367,** 467–473.

Raybuck S. A., Distefano M. D., Teo B. K., Orme-Johnson W., and Walsh C. T. (1990) An EXAFS investigation of Hg(II) binding to mercuric reductase: comparative analysis of the wild-type enzyme and a mutant enzyme generated by site-directed mutagenesis. *J. Am. Chem. Soc.* **112,** 1983–1989.

Rehr J. J., Booth C. H., Bridges F., and Zabinsky S. I. (1994) X-ray-absorption fine structure in embedded atoms. *Phys. Rev. B* **49,** 12347–12350.

Reid R. S. and Rabenstein D. L. (1981) Nuclear magnetic resonance studies of the solution chemistry of metal complexes XVII. *Can. J. Chem.* **59,** 1505–1514.

Ressler, T. (1997) WinXAS software for EXAFS data reduction.

Skyllberg U., Xia K., Bloom P. R., Nater E. A., and Bleam W. F. (2000) Binding of mercury (II) to reduced sulfur in soil organic matter along upland-peat soil transects. *J. Environ. Qual.* **29,** 855–865.

Smith R. M. and Martell A. E. (1993) *NIST Critical Stability Constants of Metal Complexes.* U.S. Department of Commerce, National Institute of Standards and Technology.

St. Louis V., Rudd J., Kelly C., Beaty K., Flett R., and Roulet N. (1996) Production and loss of methylmercury and loss of total mercury from boreal forest catchments containing different types of wetlands. *Environ. Sci. Technol.* **30,** 2719–2729.

Szulczewski M.D., Helmke P.A., and Bleam W.F. (2001) XANES spectroscopy studies of Cr(VI) reduction by thiols in organosulfur compounds and humic substances. *Environ. Sci. Technol.* **35,** 1134–1141.

Taylor N. J., Wong Y. S., Chieh P. C., and Carthy A. J. (1975) Syntheses, x-ray crystal structure, and vibrational spectra of L-cysteinato(methyl)mercury(II) monohydrate. *J. Chem. Soc. Dalton Trans.,* 438–442.

Tossell J. A. (2001) Calculation of the structures, stabilities, and properties of mercury sulfide species in aqueous solution. *J. Phys. Chem. A* **105,** 935–941.

Vaithiyanathan P., Richardson C. J., Kavanaugh R. G., Craft C.B., and Barkay T. (1996) Relationships of eutrophication to the distribution of mercury and to the potential for methylmercury production in the peat soils of the everglades. *Environ. Sci. Technol.* **30,** 2591–2597.

Waldo G. S., Carlson R. M. K., Moldowan J. M., Petters K. E., and Penner-Hahn J. E. (1991) Sulfur speciation in heavy petroleums - information from X-ray absorption near-edge structure. *Geochim. Cosmochim. Acta* **55,** 801–804.

Watras C. J. and Huckabee J. W. (1994) *Mercury Pollution—Integration and Synthesis.* Lewis Publishers, CRC Press.

Weesner F. J., Bohne H., and Bleam W. F. (1997) Sample shuttle for fluorescence- yield x-ray absorption detector maintains sample chamber purge atmosphere.. *Rev. Sci. Instrum.* **68,** 3597–3598.

Xia K., Bleam W. F., and Helmke P. A. (1997) Studies of the nature of Cu^{2+} and Pb^{2+} binding sites in soil humic substances using X-ray absorption spectroscopy. *Geochim. Cosmochim. Acta* **61,** 2211–2221.

Xia K., Weesher F., Bleam W. F., Bloom P. R., Skyllberg U. L., and Helmke P. A. (1998) XANES studies of oxidation states of sulfur in

aquatic and soil humic substances. *Soil Sci. Soc. Am. J.* **62,** 1240–1246.

Xia K., Skyllberg U. L., Bleam W. F., Bloom P. R., Nater E. A., and Helmke P. A. (1999) X-ray absorption spectroscopic evidence for the complexation of Hg(II) by reduced sulfur in soil humic substances. *Environ. Sci. Technol.* **33,** 257–261.

Zabinsky S. I., Rehr J. J., Ankudinov A., Albers R. C., and Eller M. J. (1995) Multiple scattering calculations of X-ray absorption spectra. *Phys. Rev. B* **52,** 2995–3009.

Zilloux E. J., Porcella D. B., and Benoit J. M. (1993) Mercury cycling and effects in freshwater wetland ecosystems.. *Environ. Toxicol. Chem.* **12,** 2245–2264.